

PREDICTING THE CONFIGURATION OF PLANETARY SYSTEM: KOI-152 OBSERVED BY KEPLER

SU WANG¹, JIANGHUI JI¹, AND JI-LIN ZHOU²*Draft version March 3, 2013*

ABSTRACT

The recent Kepler discovery of KOI-152 reveals a system of three hot super-Earth candidates that are in or near a 4:2:1 mean motion resonance. It is unlikely that they formed in situ, the planets probably underwent orbital migration during the formation and evolution process. The small semimajor axes of the three planets suggest that migration stopped at the inner edge of the primordial gas disk. In this paper we focus on the influence of migration halting mechanisms, including migration "dead zones", and inner truncation by the stellar magnetic field. We show that the stellar accretion rate, stellar magnetic field and the speed of migration in the proto-planetary disk are the main factors affecting the final configuration of KOI-152. Our simulations suggest that three planets may be around a star with low star accretion rate or with high magnetic field. On the other hand, slow type I migration, which decreases to one tenth of the linear analysis results, favors forming the configuration of KOI-152. Under such formation scenario, the planets in the system are not massive enough to open gaps in the gas disk. The upper limit of the planetary masses are estimated to be about 15, 19, and 24 M_{\oplus} , respectively. Our results are also indicative of the near Laplacian configurations that are quite common in planetary systems.

Subject headings: (stars: KIC 8394721) planetary systems: formation-solar system: formation-stars: individual (KOI-152)

1. INTRODUCTION

The Kepler Mission, launched in March 2009, photometrically monitors a large patch of sky with sufficient precision to detect terrestrial sized planets in potentially habitable orbits. The Kepler Mission has released their first 16 months data of 2321 transiting planet candidates (Batalha et al. 2012; Fabrycky et al. 2012). The mission is sensitive to a larger range of semimajor axes than ground-based transit surveys (Borucki et al. 2010). Thus there are opportunities to detect multiplanetary systems. According to statistical results on the first four months data, $\sim 17\%$ systems have multiple planet candidates (Borucki et al. 2011). More than a dozen multiple transiting planet systems will be confirmed or rejected by means of transit timing variations (TTVs) (Ford et al. 2011). The candidate multiple planetary systems show that at least $\sim 16\%$ contain a pair of planets close to 2:1 period commensurability (with a period ratio of two planets ranging from 1.83 to 2.18) (Lissauer et al. 2011). Furthermore, the detailed statistical analysis of the release data over 16 months suggests that the fraction of multiple planetary systems has raised from 17% to 20% and the number of the resonant systems also increases (Batalha et al. 2012). The resonant systems are of value to the researchers, who investigate formation and evolution of the planetary systems. Steffen et al. (2010) analyzed five Kepler target stars and their planet candidates, in which KOI-152 (KOI: Kepler Objects of Interest) is a known system, consisting of three planetary candidates. Moreover, three planets, orbiting about an F dwarf star (KIC 8394721) with a mass of $1.4 M_{\odot}$, are very close

to 4:2:1 mean motion resonance (MMR) (Steffen et al. 2010). Table 1 shows the orbital elements of the planets in some detail, i.e., 152.01, 152.02, and 152.03 in the order that the transit detection software identified them in the Kepler data, and hereafter we label them as Planet 01, 02, and 03, respectively, for brevity. Their masses are now estimated to be in the range of (20-100) M_{\oplus} , (9-30) M_{\oplus} , and (9-30) M_{\oplus} , respectively. Considering the density limit and formation scenarios, observers may assume them to be 60 M_{\oplus} , 15 M_{\oplus} , and 15 M_{\oplus} , respectively. Although the semimajor axis of Planet 01 is not well determined, estimated value indicates that they are very close to the central star. The orbital period ratios of each pairs are $P_{02}/P_{03} \simeq 2.033$ and $P_{01}/P_{02} \geq 1.896$. The eccentricities are estimated to be zero and no evidence for large eccentricities has been revealed (Steffen et al. 2010). Therefore, we assume the eccentricities to be zero in this work. Based on the possibility of observing such a three-planet system, the planets likely occupy nearly coplanar orbits with a small deviation of inclination from fundamental framework (Steffen et al. 2010).

It is well-known that the planetary configurations involved in 4:2:1 MMR, also occur both in our solar system and exoplanetary systems. For instance, the Galilean moons of Jupiter had been revealed in a three-body Laplace resonance over several hundred years. In addition, another example is that three super-Earths constitute the HD 40307 system, where three planets are near 4:2:1 MMRs (Papaloizou & Terquem 2010), similar to KOI-152. For HD 40307, three proto-planets formed in the proto-planetary disk with configuration near MMRs, which strongly constrains the planetary formation and orbital migration theories. In this sense, the formation scenario of such near Laplacian configuration is of great interest to the researchers, and such investigations may test some planetary formation theory.

According to core-accretion model, a planet with semi-

¹ Purple Mountain Observatory, Chinese Academy of Sciences, Nanjing 210008, China; wangsus@pmo.ac.cn, jijh@pmo.ac.cn.

² Department of Astronomy & Key Laboratory of Modern Astronomy and Astrophysics in Ministry of Education, Nanjing University, Nanjing 210093, China.

major axis a can grow up with the material surrounding it to mass m_{iso} (Ida & Lin 2004)

$$M_{\text{iso}} \simeq 0.16 f_d^{3/2} \gamma_{\text{ice}}^{3/2} \left(\frac{\Delta_{\text{fz}}}{10 R_h} \right)^{3/2} \left(\frac{a}{\text{AU}} \right)^{3/4} \left(\frac{M_*}{M_\odot} \right)^{-1/2} M_\oplus, \quad (1)$$

where $R_h = (m/3M_*)^{1/3}a$ is the Hill radius of a planet with a mass m , and $\Delta_{\text{fz}} \sim 7 - 10 R_h$ is the so-called feeding zone of the planet, M_* is the mass of central star, f_d is the enhancement factor to the Minimum Mass Solar Nebula (MMSN), γ_{ice} is the volatile enhancement for exterior or interior to the snow line a_{ice} with a value of 4.2 or 1, respectively. For KOI-152, we adopt $a_{\text{ice}} = 5.29$ AU (Ida & Lin 2004). If three planets formed in the region as shown in Table 1 with their estimated minimum masses, f_d should be at least 37. Hence, we may conclude that it is impossible that all planets formed *in situ*.

Now, it is widely believed that there are mainly two formation mechanisms to produce short-period planets, e.g., planet-planet scattering and planetary migration (Rasio & Ford 1996). The planet-planet scattering scenario always requires a massive planet to stir up the eccentricities of other bodies and trigger the scattering process. After this process had done, some planets may obtain high eccentricity (Rasio & Ford 1996), away from their initial locations. However, the planets of KOI-152 are near 4:2:1 MMR with nearly circular orbits, and in this sense it seems to be impossible to tune scattering scenario to yield such a precise configuration.

Another mechanism is that the orbital migration occurs in the gaseous disk (Goldreich & Tremaine 1980; Lin et al. 1996). Multiple planets are likely to be captured into MMRs given an appropriate migration speed (Masset & Snellgrove 2001). As MMR commonly emerges in the planetary systems, the orbital migration is now considered as one of the plausible mechanisms to form such systems. Take the GJ 876 system as an example, consisting of four planets, GJ 876 b and GJ 876 c are locked into 2:1 MMR, which can be explained by migration scenario (Lee & Peale 2002; Ji et al. 2002, 2003; Zhou et al. 2005; Zhang et al. 2010).

Recently, an alternative scenario of collision-merger has been proposed to account for the formation of short-period planets (Ji et al. 2011). In this mechanism, several embryos can be excited by giant planets after the gas of the disk depletes, and then merge into a larger body moving on a close-in orbit. Nevertheless, in these scenarios, planets are not easy to form in MMRs.

Considering the aforementioned factors, we propose a scenario to produce a configuration of KOI-152. First, three planets are assumed to have formed in the region away from the star with their nominal masses. Then, the planets may undergo type I or II migration due to interaction with the gaseous disk until they halt at the inner region of the disk. In this phase, three planets are trapped into MMRs during the migration. Finally, tidal effects, arising from the central star, circularizes their orbits.

Such a scenario had been supposed by Terquem & Papaloizou (2007). They calculated a series of runs that are composed of 10-25 planets or planetary cores in a disk with masses ranging from 0.1 to 1 M_\oplus , which undergo type I migration. They showed that hot super-Earths or Neptunes do not

become isolated during their inward migration, and the companions on near-commensurate orbits always survive. Nevertheless, in their work, the authors did not consider the effect of different speed of type I migration, which can occur. In a more recent work, Papaloizou & Terquem (2010) investigated the formation of the HD 40307 system, bearing a resemblance to KOI-152. They adopted a similar formation scenario and found that in the end of the simulations, the planets are driven out of Laplace resonances due to tidal effects with the central star, and they finally reach a planetary configuration very close to HD 40307. Furthermore, Wang & Zhou (2011) accounted for the contribution of type I migration and mainly focused on the speed of migration under the perturbation of gas-giants in the outer region in M dwarf system. They further point out that pairs of planets favor forming not only near the 2:1 MMR but other first order resonances.

One of the important factors that influence final configurations is holes in the gas disk. In general, holes can appear at two positions. One is the boundary of the dead zone and the active zone in the midplane of the disk responding to the magnetorotational instability (MRI). For protostellar gas disk in ad hoc α -prescription (Shakura & Sunyaev 1973), the mass accretion rate, $\dot{M}_g = 3\pi\alpha c_s h \Sigma_g$, is constant across the whole disk, where $h = c_s/\Omega_k$ is the disk scale height, c_s , Ω_k , and Σ_g are the sound speed of the midplane, the Kepler angular velocity, and the gas density, respectively. As the value of α decreases from the active zone (~ 0.018 ; Sato et al. 2000) to the dead zone (~ 0.006), in the midplane the value of the gas density in the dead zone (outer) is three times of that in the active zone (inner). Then a maximum density location occurs. Another is the inner hole of the disk caused by the coupling of the star's magnetic field with the gas. Gas falls onto the surface of the central star under the effect of the torque induced by the stellar magnetic field, a truncation happens at the inner region and an inner hole appears. A maximum density of the gas disk appears at the boundary of the inner hole. Due to the variation of density, the speed of type I migration may be changed. The two mentioned regions play a significant role in forming the final planetary configuration, especially for low-mass planetary systems.

In this work, we focus on exploring the configuration formation of KOI-152, mainly on the following aspects: (a) the speed of type I migration of planets, (b) the density profile of gas disk, (c) the possible range of masses of three planets, and (d) the nature of the star in the system. This paper is organized as follows: In §2, we introduce the adopted disk model, orbital migration and eccentricity damping models in the investigation. In §3., we present the simulation method and outcomes. Finally, we conclude and summarize the results in §4.

2. MODELS

2.1. Disk Model

In order to explore the configuration formation, we consider a system consisting of a central star and three planets, which formed far away from the star. We assume that three planets are initially embedded in a gaseous

TABLE 1
ORBITAL PARAMETERS OF THE KOI-152 PLANETARY SYSTEM.

ID	Semimajor axis (AU)	Period (day)	Eccentricity	Mass (M_{\oplus})
152.03	0.124	13.48	0.00	15
152.02	0.199	27.40	0.00	15
152.01	0.305	≥ 51.94	0.00	60

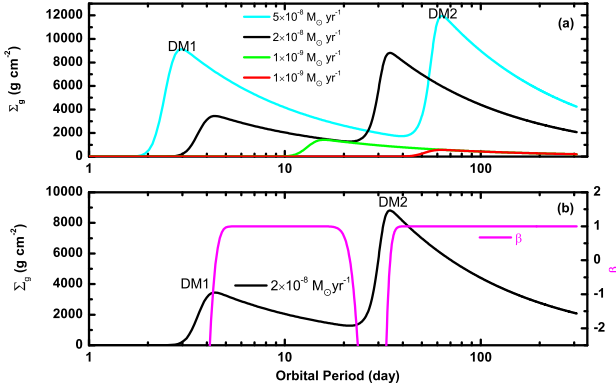


FIG. 1.— The density profile of the gas disk and the values of β . The upper panel (a) shows the gas density profile with star accretion rate ($\dot{M} = [1 \times 10^{-9}, 5 \times 10^{-8}] M_{\odot} \text{ yr}^{-1}$), $\alpha_{\text{dead}} = 0.001$, and $\alpha_{\text{mri}} = 0.01$. The parameters of the star are set to be $B_* = 0.5$ KG and $R_* = 2.5 R_{\odot}$ except the red line for the cases in Group 4 with high magnetic field $B_* = 2.5$ KG. The bottom panel (b) illustrates the values of β , taking $\dot{M} = 2 \times 10^{-8} M_{\odot} \text{ yr}^{-1}$ as an example. Two maximum density locations at ~ 3.6 days and 26 days, respectively, where β changes from positive to negative at DM2 and the region inside DM1.

disk. The surface density is given as (Pringle 1981)

$$\Sigma_g = \frac{\dot{M}}{3\pi\nu(a)}, \quad (2)$$

where \dot{M} is the accretion rate of the star and $\nu(a)$ is the effective viscosity at the orbit of a semimajor axis a . According to the observation of young cluster ρ -Oph, the accretion rate of the star can be written as (Natta et al. 2006; Vorobyov & Basu 2009)

$$\dot{M} \simeq 2.5 \times 10^{-8} \left(\frac{M_*}{M_{\odot}} \right)^{1.3 \pm 0.3} M_{\odot} \text{ yr}^{-1}. \quad (3)$$

According to equation (3), the accretion rate of star is $\sim 3.87 \times 10^{-8} M_{\odot} \text{ yr}^{-1}$ for this system. Nevertheless, the value will decrease, on average, with the evolution of T Tauri star and its disk. Hence, herein we consider the star accretion rate in the range of $[1 \times 10^{-9}, 5 \times 10^{-8}] M_{\odot} \text{ yr}^{-1}$. The effective viscosity of the disk is $\nu(a) = \alpha c_s h$, where α and c_s , represent the efficiency factor of angular momentum transport, and sound speed at the midplane, respectively; $h = c_s/\Omega$ means the isothermal density scale height, Ω refers to the Kepler angular velocity (Shakura & Sunyaev 1973). Because of the effect of MRI, the values of α in the active zone and the dead zone are quite different. The effective value of α is

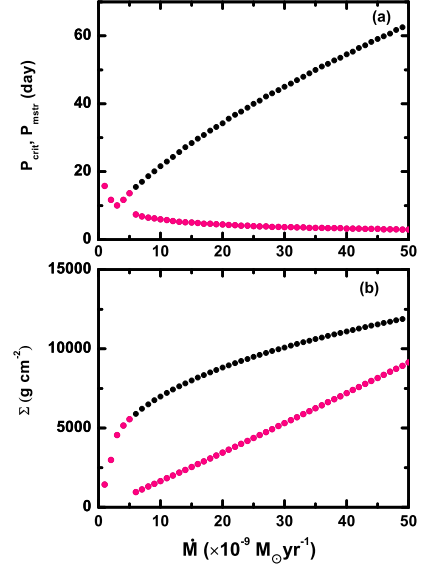


FIG. 2.— The relationship between the gas density and star accretion rate. The upper panel (a) shows the orbital period at the location of maximum density with various star accretion rate. The black dot line represents the boundary of the dead zone and the active zone using equation (5) while the purple line indicates the truncated location according to equation (7). The bottom panel (b) displays the values of density at two maximum density locations.

expressed as (Kretke & Lin 2007; Kretke et al. 2009)

$$\alpha_{\text{eff}}(a) = \frac{\alpha_{\text{dead}} - \alpha_{\text{mri}}}{2} \left[\text{erf} \left(\frac{a - a_{\text{crit}}}{0.1a_{\text{crit}}} \right) + 1 \right] + \alpha_{\text{mri}}, \quad (4)$$

where α_{mri} , α_{dead} denote the value of α in active zone and dead zone, respectively. Herein, we choose $\alpha_{\text{dead}} = 0.001$ and $\alpha_{\text{mri}} = 0.01$ (Sano et al. 2000). The parameter a_{crit} in the error function erf is the location of the boundary of MRI and $0.1a_{\text{crit}}$ represents the width of the transition zone. a_{crit} is modeled as (Kretke et al. 2009)

$$a_{\text{crit}} = 0.16 \text{ AU} \left(\frac{\dot{M}}{10^{-8} M_{\odot} \text{ yr}^{-1}} \right)^{4/9} \left(\frac{M_*}{M_{\odot}} \right)^{1/3} \times \left(\frac{\alpha_{\text{mri}}}{0.02} \right)^{-1/5} \left(\frac{\kappa_D}{1 \text{ cm}^2 \text{ g}^{-1}} \right), \quad (5)$$

where κ_D is the grain opacity.

Considering the disk depletion, the gas density profile can be modified to be

$$\Sigma_g = \frac{\dot{M}}{3\pi\nu(a)} \exp \left(-\frac{t}{\tau_{\text{dep}}} \right), \quad (6)$$

where τ_{dep} refers to the disk depletion timescale, which is observed as few million years (Haisch et al 2001). We adopt $\tau_{\text{dep}} = 10^6 \text{ yr}$ in the simulations, where t is the time of evolution.

Because of the stellar magnetic field, the gas disk is truncated at a_{mstr} (Koenigl 1991)

$$a_{\text{mstr}} = (1.06 \times 10^{-2} \text{ AU}) \beta' \left(\frac{R_*}{R_\odot} \right)^{12/7} \left(\frac{B_*}{1000\text{G}} \right)^{4/7} \times \left(\frac{M_*}{M_\odot} \right)^{-1/7} \left(\frac{\dot{M}}{10^{-7} M_\odot \text{ yr}^{-1}} \right)^{-2/7} \quad (7)$$

where R_* , R_\odot , and B_* refer to the radius of the star, the radius of the sun and the magnetic field of the central star, respectively. $\beta' \leq 1$ is a free parameter. Herein, we choose $\beta' = 1$ corresponding to a typical Alfvén radius in the way of spherical accretion. Hereafter we use P_{crit} and P_{mstr} , the Keplerian orbital period, instead of a_{crit} and a_{mstr} for convenience. Combining the effect of the magnetic field, the gas density profile is substituted by

$$\Sigma_g = \frac{\dot{M}}{3\pi\nu(a)} \exp\left(-\frac{t}{\tau_{\text{dep}}}\right) \eta, \quad (8)$$

where

$$\eta = 0.5 \left[\text{erf}\left(\frac{a - a_{\text{mstr}}}{0.1 a_{\text{mstr}}}\right) + 1 \right], \quad (9)$$

is induced by the truncation of the magnetic field.

Based on equation (8), we find that $\Sigma_g \propto r^{-1}$ and there are generally two maxima in the gas density profile. Figure 1 shows the density profile with various star accretion rates (see the top panel (a)). We label the inner maximum density location as DM1, similarly, the outer one as DM2. The locations of DM1 and DM2 change with the star accretion rate. In Figure 2 we show the density versus star accretion rate. From Figure 2 (the top panel (a)), we notice that, with a decrease of star accretion rate, the values of DM1 and DM2 approach each other until they merge into one, the combination occurs at $\sim \dot{M} = 5 \times 10^{-9} M_\odot \text{ yr}^{-1}$, corresponding to a maximum density at an orbital period of 13 days. Herein we choose $\alpha_{\text{dead}} = 0.001$, $\alpha_{\text{mri}} = 0.01$, and $B_* = 0.5 \text{ KG}$, respectively, where the bottom panel (b) displays the values of the density at DM1 and DM2, respectively.

2.2. Planetary migration and eccentricity damping

For the planets in KOI-152 system, their masses are estimated to be less than $100 M_\oplus$. From a classical planetary formation theory, they may undergo type I or type II migration during their evolution.

Type I migration is induced by angular-momentum exchange between gas disk and planets. Based on linear analysis, the net momentum loss on a planet causes an inward migration (Goldreich & Tremaine 1979; Ward 1997; Tanaka et al. 2002). Under this assumption, the speed of type I migration is very fast. In such situation, it is difficult to produce terrestrial planets. Recently, there are several new theories on reducing the speed of type I migration or even reverse the migrating direction (Baruteau & Masset 2008; Kley & Crida 2008; Kley et al. 2009; Paardekooper & Papaloizou 2008; Wang & Zhou 2011).

Considering the uncertainty of type I migration, we adopt a reduction of the migration speed, taking a timescale of type I migration of an embryo with mass

m as (Tanaka et al. 2002)

$$\tau_{\text{migI}} = \frac{a}{|\dot{a}|} = \frac{1}{f_1} \tau_{\text{linear}} = \frac{1}{f_1(2.7 + 1.1\beta)} \left(\frac{M_*}{m} \right) \left(\frac{M_*}{\Sigma_g a^2} \right) \times \left(\frac{h}{a} \right)^2 \left[\frac{1 + \left(\frac{er}{1.3h} \right)^5}{1 - \left(\frac{er}{1.1h} \right)^4} \right] \Omega^{-1} \text{yr}, \quad (10)$$

where e , r , h , and Ω are eccentricity, distance from the central star, scale height of the disk, and the Keplerian angular velocity, respectively. τ_{linear} is the timescale of linear analysis result, f_1 is the reduction factor. Herein, we choose $f_1 = 0.03$, 0.1 , and 0.3 , respectively, and $\beta = -d \ln \Sigma_g / d \ln a$. Σ_g means the gas density profile of the disk expressed in equation (8). As the value of β is related to the density profile, the speed of type I migration may be slowed down or even reversed at some special areas. In addition, Figure 1 shows the values of β using $\dot{M} = 2 \times 10^{-8} M_\odot \text{ yr}^{-1}$ as an example (see the bottom panel (b)). According to equation (10), if $\beta < -2.45$, the timescale of type I migration will transfer from positive to negative. Furthermore, we notice that when embryos run across DM2 and DM1, the migration speed will decrease, which may lead to the trapping of the embryos there.

When it grows massive enough, a planet will start to experience type II migration, as the strong torque caused by the planet will open a gap in the gaseous disk (Lin & Papaloizou 1993). The timescale of type II migration for a planet with mass m is (Ida & Lin 2008)

$$\tau_{\text{migII1}} \simeq 5 \times 10^5 f_g^{-1} \times \left(\frac{C_2 \alpha}{10^{-4}} \right)^{-1} \left(\frac{m}{M_J} \right) \left(\frac{a}{1 \text{AU}} \right)^{1/2} \left(\frac{M_*}{M_\odot} \right)^{-1/2} \text{yr},$$

$$\tau_{\text{migII2}} = \frac{a}{|\dot{a}|} = 0.7 \times 10^5 \left(\frac{\alpha}{10^{-3}} \right)^{-1} \left(\frac{a}{1 \text{AU}} \right) \left(\frac{M_*}{M_\odot} \right)^{-1/2} \text{yr}, \quad (11)$$

where α is the efficiency factor of angular momentum transport. When the mass of planet is comparable to that of the gas disk, a fraction ($C_2 \sim 0.1$) of total angular momentum will transfer between the planet and the disk in the evolution. In this case, τ_{migII1} applies. Herein we adopt $\alpha = \alpha_{\text{dead}} = 0.001$, $C_2 \alpha = 10^{-4}$. If the mass of the gas disk is larger than that of the planet, it will migrate with the gas disk over the timescale of τ_{migII2} . We emphasize that the timescale of type II migration is larger than that of type I.

A gap will form in the gas disk when the planet grows to massive enough ($m > M_{\text{crit}}$) (Ida & Lin 2008),

$$M_{\text{crit}} \simeq 30 \left(\frac{\alpha}{10^{-3}} \right) \left(\frac{a}{1 \text{AU}} \right)^{1/2} \left(\frac{M_*}{M_\odot} \right) M_\oplus. \quad (12)$$

In this work, we assume that the planet will undergo type II migration when its mass is greater than M_{crit} .

Additionally, we consider the eccentricity damping induced by the interactions between the gas disk and embryo (Goldreich & Tremaine 1979). The damping timescale for an embryo with mass m is described as (Cresswell & Nelson 2006)

$$\tau_e = \left(\frac{e}{\dot{e}} \right)_{\text{edamp}} = \frac{Q_e}{0.78} \left(\frac{M_*}{m} \right) \left(\frac{M_*}{a^2 \Sigma_g} \right) \left(\frac{h}{r} \right)^4 \Omega^{-1} \times \left[1 + \frac{1}{4} \left(\frac{er}{h} \right)^3 \right] \text{yr}, \quad (13)$$

where $Q_e = 0.1$ is a normalization factor to be consistent with hydrodynamical simulations. The meanings of other symbols are similar to those in equation (10).

3. NUMERICAL SIMULATIONS AND RESULTS

To explore the secular evolution of the KOI-152 planetary system, we assume that three planets had formed in the outer region of the system and migrate toward the inner region due to the interactions with the gas disk. Thus, the acceleration of a planet with mass m_i is given as

$$\frac{d}{dt}\mathbf{V}_i = -\frac{G(M_* + m_i)}{r_i^2} \left(\frac{\mathbf{r}_i}{r_i} \right) + \sum_{j \neq i} Gm_j \left[\frac{(\mathbf{r}_j - \mathbf{r}_i)}{|\mathbf{r}_j - \mathbf{r}_i|^3} - \frac{\mathbf{r}_j}{r_j^3} \right] + \mathbf{F}_{\text{edamp}} + \mathbf{F}_{\text{migI}}(\text{or } + \mathbf{F}_{\text{migII}}), \quad (14)$$

where \mathbf{r}_i and \mathbf{V}_i mean the position and velocity vectors of the planet m_i in the stellar-centric coordinates, and the external forces are defined as

$$\begin{aligned} \mathbf{F}_{\text{edamp}} &= -2 \frac{(\mathbf{V}_i \cdot \mathbf{r}_i) \mathbf{r}_i}{r_i^2 \tau_e}, \\ \mathbf{F}_{\text{migI}} &= -\frac{\mathbf{V}_i}{2\tau_{\text{migI}}}, \\ \mathbf{F}_{\text{migII}} &= -\frac{\mathbf{V}_i}{2\tau_{\text{migII}}}. \end{aligned} \quad (15)$$

Each planet is assumed to be initially in coplanar and near-circular orbit and suffers from mutual gravitational interaction and the effect exerted by the central star. The initial orbital elements of each planet were randomly generated: argument of pericentre, longitude of the ascending node, and mean anomaly were randomly set between 0° to 360° . In this way, we generate a set of 34 runs for simulation.

We numerically integrate the equations (14) using a time-symmetric Hermit scheme (Aarseth 2003). If the distance from a planet to the central star is smaller than the radii of the star we originally set, we assume that the planet collides with the star. Each run evolved for 10^8 yr.

Based on equation (12), for $\alpha = 10^{-3}$, if $a > 0.125$ AU, then we have $M_{\text{crit}} > 15 M_\oplus$. Hence, if their initial locations are all without 0.125 AU, KOI-152.02 and KOI-152.03 will undergo type I migration, the outmost one will experience type I or II migration. In this sense, two kinds of models are assumed in the simulations: For Model 1, we suppose that all planets will suffer type I migration; whereas for Model 2, we simply consider that KOI-152.02 and KOI-152.03 will go through type I migration but KOI-152.01 will undergo type II migration. According to the aforementioned analysis, one of the planets in this system may be captured at DM1 or DM2. In such case, taking into account the range of the star accretion rate $[1 \times 10^{-9}, 5 \times 10^{-8}] M_\odot \text{ yr}^{-1}$, we find that the positions of DM2 are at $\sim 13, 26$, and 48 days, respectively, in three groups for Model 1. In addition, the conditions of density profile of various groups and models are summarized as follows.

Model 1

Group 1: For $\dot{M} = 5 \times 10^{-8} M_\odot \text{ yr}^{-1}$, the density profile Σ_g is labeled as the blue line in Figure 1. DM2 = 48.039 days, KOI-152.01 is likely to be captured at a_{crit} .

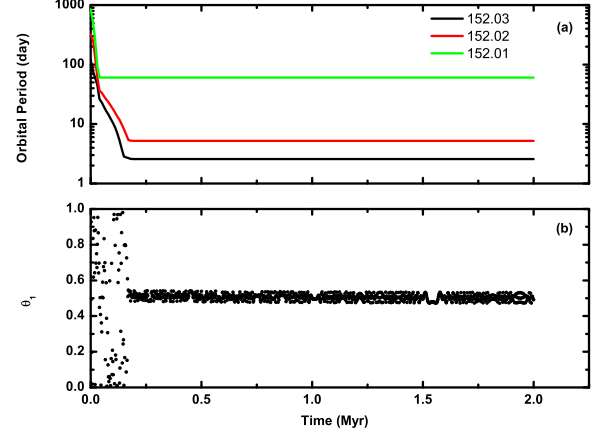


FIG. 3.— The evolution of orbital periods and resonant angle in Group 1. At ~ 0.2 Myr, KOI-152.02 and KOI-152.03 are evolved into a 2:1 MMR in the evolution. The upper panel (a) shows the time evolution of the orbital periods. Planet 03 halts at DM2 first until Planet 02 comes. Planet 02 kicks 03 into the inner region when it migrates towards DM2 and the outmost planet keeps Planet 02 repeating this process just as the first two planets do. At the end of the run, Planet 03 stops at DM1. The bottom panel (b) shows one of the 2:1 resonant angles of Planet 02 and 03. (Hereafter, we label $\theta_1 = 2\lambda_{02} - \lambda_{03} - \varpi_{02}$, $\theta_2 = 2\lambda_{02} - \lambda_{03} - \varpi_{03}$, $\theta_3 = 2\lambda_{01} - \lambda_{02} - \varpi_{01}$, $\theta_4 = 2\lambda_{01} - \lambda_{02} - \varpi_{02}$.)

Group 2: For $\dot{M} = 2 \times 10^{-8} M_\odot \text{ yr}^{-1}$, Σ_g is labeled as the black line (Figure 1). DM2 = 26.08 days, KOI-152.02 is likely to be captured at a_{crit} .

Group 3: For $\dot{M} = 1 \times 10^{-9} M_\odot \text{ yr}^{-1}$, Σ_g is labeled as the green line (Figure 1). DM2 = 13.067 days, KOI-152.03 is likely to be captured at a_{crit} .

Group 4: For $\dot{M} = 1 \times 10^{-9} M_\odot \text{ yr}^{-1}$, Σ_g is labeled as the red line (Figure 1). DM2 = 51.9 days, KOI-152.01 is likely to be captured at a_{crit} .

Model 2

Comparison with Group 2 of Model 1: For $\dot{M} = 2 \times 10^{-8} M_\odot \text{ yr}^{-1}$, Σ_g labeled as the black line in Figure 1. DM2 = 26.08 days, KOI-152.02 is likely to be captured at a_{crit} . However, KOI-152.01 will undergo type II migration.

3.1. Model 1: All planets undergo type I migration

In order to understand the influence of the star accretion rate and the speed of type I migration, we perform four groups of simulations. Table 2 are listed the detailed information for the dominant results of each group, where the last column shows the Keplerian orbital periods at the locations of DM1 and DM2.

3.1.1. Group 1: KOI-152.01 captured at a_{crit}

In this group, DM1 and DM2 occur at ~ 2.4 days and 48 days, separately, with $\dot{M} = 5 \times 10^{-8} M_\odot \text{ yr}^{-1}$. From the profile of gas density, we note that, if Planet 01 is likely to be trapped at DM2, the resulting configuration may be analogous to KOI-152. In total, we performed five runs to examine how the planets come into the resonant region, where Table 2 reports typical outcomes in our simulations. For example, in a typical run, Planet 02 or 03 will continue to move inward until reaching DM1 in

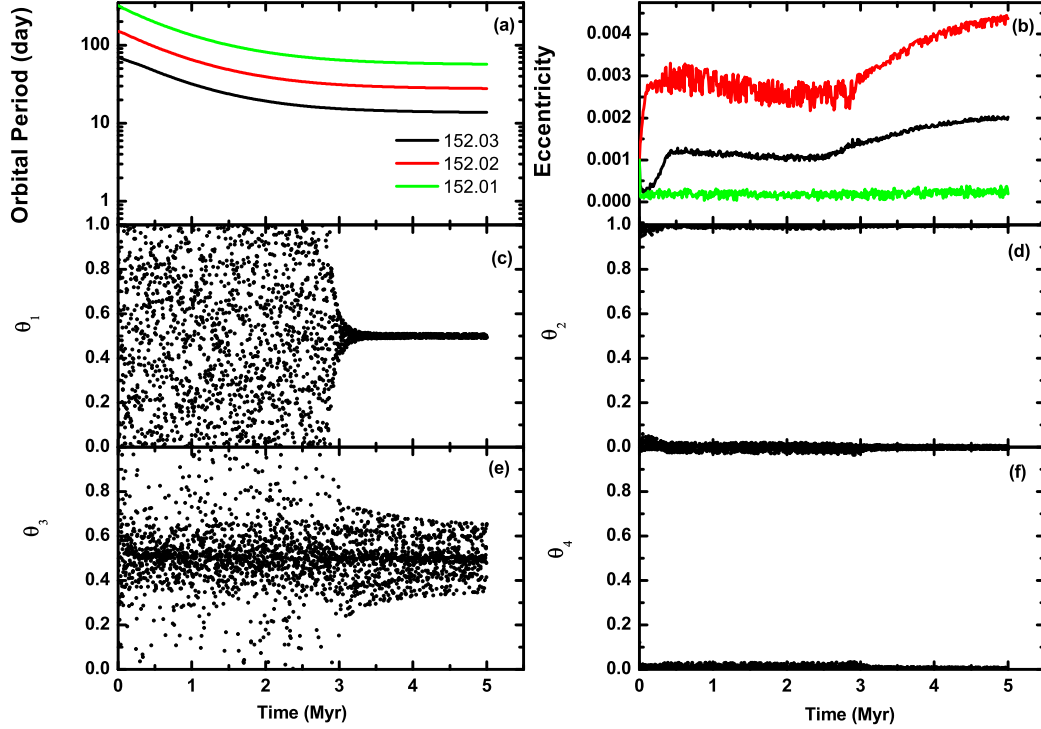


FIG. 4.— The results of the evolution for Group 3-2. The two upper panels (a and b) show the evolution of orbital periods and eccentricities. The middle and bottom panels (c-f) are indicative of the resonant angles of three planets. In this run, they are captured into 4:2:1 MMR over very shorter timescale. In the end of this run, a planetary configuration similar to KOI-152, which consists of three planets, is formed.

TABLE 2

DETAILED INFORMATION OF FIVE GROUPS IN THE SIMULATIONS. TERMINAL PERIODS ARE THE ORBITAL PERIODS OF THREE PLANETS AT THE END OF RUN. P_{crit} AND P_{mstr} REPRESENT KEPLERIAN ORBITAL PERIODS IN ASSOCIATION WITH THE REGIME OF DM1 AND DM2.

ID	\dot{M} ($M_{\odot} \text{ yr}^{-1}$)	Initial periods (days)	f_1	Terminal periods (days)	Terminal periods ratios ($P_{01}/P_{02}, P_{02}/P_{03}$)	$P_{\text{crit}}, P_{\text{mstr}}$ (days)
Group 1	5×10^{-8}	120, 320, 850	0.1	2.58, 5.2, 60.5	11.63, 2.02	48.039, 2.443
Group 2-1	2×10^{-8}	120, 320, 850	0.03	3.8, 7.75, 32.83	4.24, 2.04	26.08, 3.618
Group 2-2	2×10^{-8}	120, 320, 850	0.1	1.899, 12.19, 24	1.97, 6.42	26.08, 3.618
Group 2-3	2×10^{-8}	120, 320, 850	0.3	3.8, 7.67, 32.85	4.28, 2.02	26.08, 3.618
Group 2-4	2×10^{-8}	120, 320, 20012	0.03	31.72, 64.23, 6960.77	108.37, 2.02	26.08, 3.618
Group 2-5	2×10^{-8}	120, 320, 20012	0.1	3.82, 7.7, 32.85	4.27, 2.01	26.08, 3.618
Group 2-6	2×10^{-8}	120, 320, 20012	0.3	3.78, 5.72, 32.83	5.74, 1.51	26.08, 3.618
Group 3-1	1×10^{-9}	120, 320, 850	0.1	3.5, 7.12, 14.73	2.07, 2.03	13.067
Group 3-2	1×10^{-9}	70, 150, 320	0.03	13.78, 27.87, 57.07	2.05, 2.02	13.067
Group 3-3	1×10^{-9}	220, 500, 1400	0.1	11.71, 23.56, 47.64	2.02, 2.01	13.067
Group 4	1×10^{-9}	220, 320, 850	0.1	14.17, 28.56, 58.54	2.05, 2.01	51.9
KOI-152				13.48, 27.40, 52.09	1.90, 2.03	

cases where they have been kicked inside of DM2. Subsequently, Planet 01 is trapped at ~ 60 days as shown in Figure 3 and the two inner planets are eventually captured into 2:1 MMR. From Figure 1, we show that if a planet is pushed into the region inside DM2, the value of β changes from negative to positive before it approaches DM1. The change in sign of β is the reason that the two inner bodies migrate towards DM1. However, no matter how we varied the speed of type I migration or re-scaled

the initial position of Planet 01, (e.g., much more distant than the value given in Table 2), Planet 02 and 03 still rush into the inner zone about DM1 in the evolution. Hence, we may safely conclude that a configuration like KOI-152 cannot be generated when the star is too young with high star accretion rate. To sum up the above outcomes, for five runs, we find that Planet 02 and 03 are locked into 2:1 MMR in three cases during dynamical evolution, whereas they are captured into 3:2 MMR in

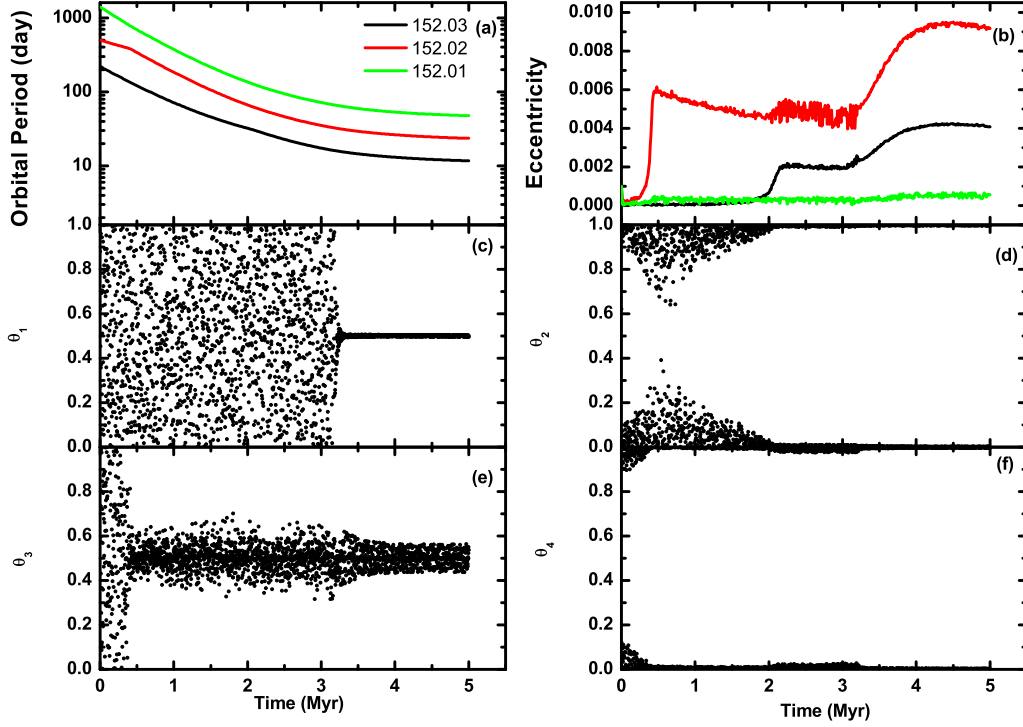


FIG. 5.— The results of the evolution Group 3-3. The two upper panels (a and b) show the evolution of orbital periods and eccentricities. The middle and bottom panels (c-f) exhibit their resonant angles. In this run, they are captured into 4:2:1 MMR within a shorter timescale. A planetary configuration analogous to KOI-152, consisting of three planets, is generated.

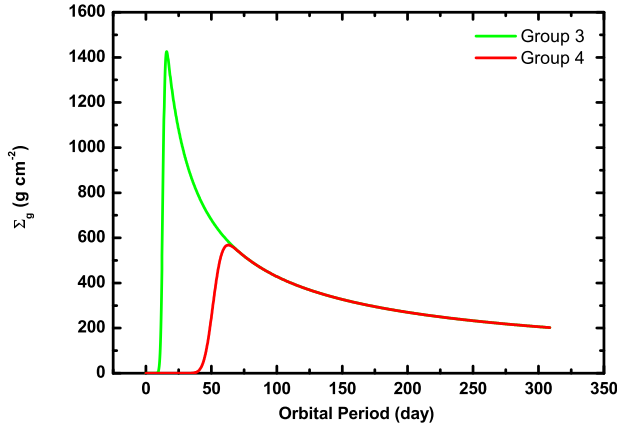


FIG. 6.— The gas density profile in Group 3 and 4. Because of a high magnetic field of the star, the gas disk will be truncated at distant region with low gas density in Group 4.

the other two runs.

In this scenario, a planetary configuration is finally created, that consists of two planets trapped into a 2:1 MMR or 3:2 MMR at DM1 and the outmost one resided inside DM2, far away from DM1.

3.1.2. Group 2: KOI-152.02 captured at a_{crit}

By adopting $\dot{M} = 2 \times 10^{-8} M_{\odot} \text{ yr}^{-1}$, we have DM1 and DM2 located at $\sim 3.6, 26$ days, respectively. In this group, we performed six runs in total. The results of all runs are reported in Table 2. From Table 2, we observe that, similar to the cases of Group 1, Planet 03 is quickly captured at DM1 as it is thrown into the region inside DM2. In Run 1-3, we utilize the same initial conditions but choose a variational migration speed. In these runs, Planet 02 cannot stay at DM2 but is kicked into the inner region by the perturbation of Planet 01, then it falls into MMR with Planet 01 (run 2) or Planet 03 (run 1, 3). In Run 4-6, Planet 01 is initially well separated from the other two, by placing the outer planet in a starting location of much more distant from the central star. The results of Run 5 and 6 are analogous to that of Run 1-3. The variation of β is the governing reason for the evolution of Run 1-3 and 5-6. However, owing to slow migration speed, Run 4 differs from other runs, where three planets cannot pass through DM2. Here, one may notice that it is impossible for three planets to form a configuration resembling to KOI-152. From the analysis of six runs, we summarize the simulation outcomes, where Planet 02 and 03 are in a 2:1 MMR for four runs and in one run they are captured into a 3:2 MMR, whereas in another special case Planet 01 and 02 become trapped into a 2:1 MMR over the evolution.

The created configuration in Group 2 varies with the

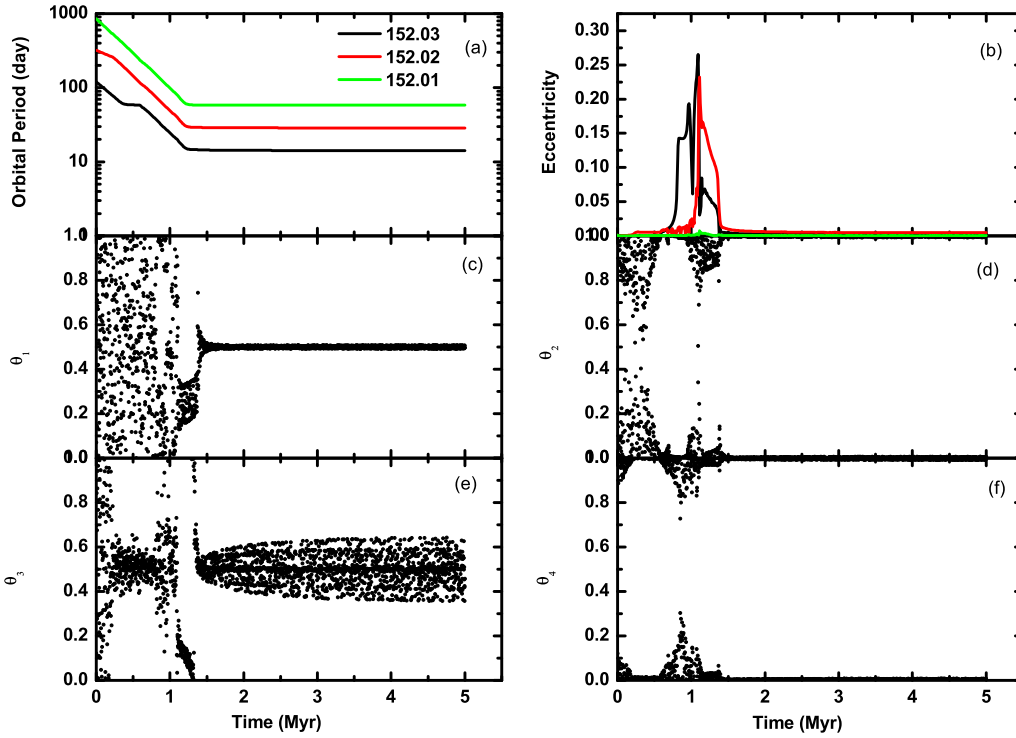


FIG. 7.— The results of the evolution for Group 4. The magnetic field is $B_* = 2.5$ KG. Note that three planets are captured into 4:2:1 MMR. The middle and bottom panels (c-f) show the time variations of their resonant angles.

value of f_1 . The inner planet is always trapped in the boundary of the inner hole unless they undergo a lower speed of type I migration and the outmost planet is formed farther simultaneously. Thus, in such scenario, a configuration similar to KOI-152 cannot be created.

3.1.3. Group 3: KOI-152.03 captured at a_{crit}

In the simulations, we assume the star accretion rate is equal to $1 \times 10^{-9} M_{\odot} \text{ yr}^{-1}$. From the density profile shown in Figure 1, we see that DM1 and DM2 tend to combine into one position at ~ 13 days. In this group, we totally carried out 10 runs. Details of three runs are also shown in Table 2. If we examine the type I migration considering $f_1 \geq 0.1$, the results of evolution then bear resemblance to the case of Group 3-1, where KOI-152.01 is trapped at ~ 14 days in the meantime the other two planets jump into the inner region at $P < 10$ days, unless we started them at distant orbits from the star or slow down the speed of type I migration. In Group 3-2, we lower the migration speed and the result is shown in Figure 4, where Planet 03 is capable to being trapped at ~ 14 days. The simulation results are consistent with the current observational values of KOI-152. When Planet 02 and 01 keep pace with Planet 03, two pairs are all captured into 2:1 MMRs. Group 3-3 simulates the condition related to a high speed of type I migration and distant initial orbits. Figure 5 displays that Planet 01 and 02 are locked into 2:1 MMR in the dynamical evolution as well as Planet 02 and 03. In conclusion, according

to our evaluation, three planets are eventually captured into Laplace resonance, with the resonant angles in a libration about 180° for Group 3-2 and 3-3. When the planets are trapped into MMRs, their eccentricities are excited during the evolution; but due to strong gas damping, they cannot be pumped up to large values.

Taking $f_1 \leq 0.1$ into account, a configuration similar to KOI-152 is formed, where two pairs of planets are in the 2:1 MMRs.

3.1.4. Group 4: High magnetic field star

Herein we consider that the star bears a high magnetic field of $B_* = 2.5$ KG. In comparison with Group 3, for a high magnetic field star, the truncation of the inner hole is at ~ 50 days, farther than that a low magnetic field star as shown in Figure 6. Herein we carried out three runs. Figure 7 illustrates the results of a typical run, where the middle and bottom panels (c-f) show the resonant angles for the planets. From the figure, we note that three planets are captured into a 4:2:1 MMR at ~ 1 Myr. Simultaneously, we examine the resonant angles and find that three planets are also locked into a Laplace resonance, librating about 0° at ~ 4 Myr. When they are captured into MMR, Planet 02 and 03 may migrate towards the inner region of the hole with little gas. Consequently, the influence of the gas damping is not dominant. Thus, the eccentricities of Planet 02 and 03 are stirred up to ~ 0.2 when they are trapped into a 2:1 MMR. However, Planet 01 remains outside the hole,

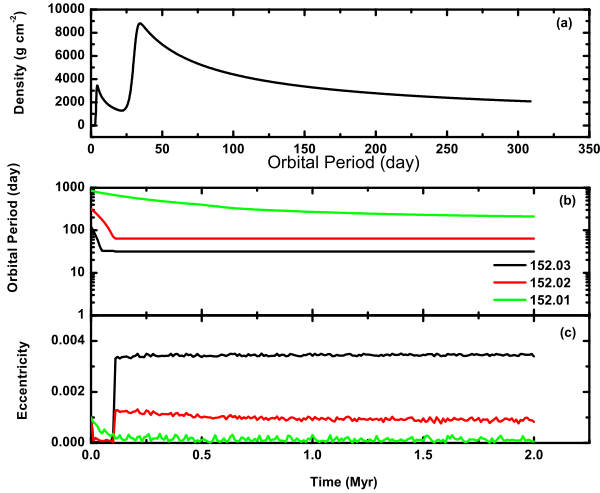


FIG. 8.— The orbital evolution for Model 2. Two inner planets undergo type I migration while the outer one suffers from type II migration. The upper panel (a) shows the density profile, and the middle and bottom panels (b and c) exhibit the time evolution of the semimajor axes and eccentricities, respectively.

and its eccentricity finally decreases to ~ 0.002 . For one paradigm, because of fast speed of type I migration, the system is totally destroyed. In another run, the produced planetary configuration is quite analogous to the typical Laplacian geometry, with the resonant angles librating at 180° . For $f_1 \leq 0.1$, we have a planetary configuration similar to KOI-152.

3.2. Model 2: KOI-152.01 undergoes type II migration

According to our above analysis, Planet 01 may perform type II migration. In this model, we set Planet 02 and 03 to undergo type I migration but Planet 01 suffers from type II migration. We carry out 10 runs for Model 2, by varying the initial position of the outmost planet. But owing to a slow speed of type II migration, Planet 01 cannot reach its nominal position even if it is placed at the orbit with a period of 70 days in the beginning. Figure 8 shows a typical run of the simulations. In this run, the density profile is the same with that in model 1 Group 2, $f_1=0.1$ for Planet 02 and 03. In the end, the simulation results show that three planets migrate to 31.72, 63.86 and 211.13 days, respectively. However, Planet 01 is a little deviated from the present-day observation.

Under this circumstance, Planet 01 cannot approach its estimated position regardless the initial location of the outmost planet. In addition, the inner two planets are always trapped into 2:1 MMR at DM2. In a word, we cannot generate a Laplacian configuration for three planets from Model 2.

4. CONCLUSIONS AND DISCUSSIONS

In this work, we have extensively investigated the formation of configuration for the KOI-152 system using numerical simulations. We assume three planets formed in a region far away from their current locations. The embedded planets in the gas disk will migrate into the regime much closer to the central star. In order to produce a configuration similar to KOI-152, there are some

requirements for the disk and the star. In summary, we reach the following conclusions:

1. If KOI-152.01 survives as predicted, no type II migration happened for three planets in the system.
2. From equation (12), the masses of three planets can be limited to be $m_{03} \leq 15$, $m_{02} \leq 19$, and $m_{01} \leq 24 M_\oplus$, respectively. According to core-accretion model, a solid core may continue to accrete gas envelope until it grows up into 2-10 M_\oplus (Barnes et al. 2009; Bodenheimer et al. 2000; Hubickyj et al. 2005; Ikoma et al. 2001; Pollack et al. 1996), therefore simply judging from the radii of the planets and the formation scenario, we cannot clearly identify the composition of the planets, and their masses are not well determined. Based on the gap opening criteria, the masses of three planets are evaluated to be (9-15) M_\oplus , (9-19) M_\oplus , and (20-24) M_\oplus , respectively.

3. Low star accretion rate and high magnetic field of the star are propitious to the formation of the configuration of KOI-152. Low star accretion rate may imply that the formation of three planets takes place at the later stage of the star evolution, where DM1 and DM2 are merged into one. From Figure 2, we learn that the boundary is about $\dot{M} = 5 \times 10^{-9} M_\odot \text{ yr}^{-1}$. In this sense, one requirement for the formation of KOI-152 is $\dot{M} \leq 5 \times 10^{-9} M_\odot \text{ yr}^{-1}$.

4. Low speed of type I migration with $f_1 \leq 0.1$ facilitates the formation of the KOI-152 system. This conclusion agrees with those mentioned by Ida & Lin (2008) and Wang & Zhou (2011).

5. In this work, we had not examined tidal interactions between planets and central star after planetary formation scenario. On the basis of tidal timescale (Mardling & Lin 2004; Zhou & Lin 2008), the eccentricities of Planet 01, 02, 03, with their nominal orbital elements will be damped in τ_{tide} , $1.3 \times 10^9 Q'$, $2 \times 10^8 Q'$, and $9.6 \times 10^6 Q'$ years, respectively, where Q' is the tidal dissipation factor and we adopt $\rho = 3 \text{ g cm}^{-3}$ for them. Meanwhile, the semimajor axes are also decreasing over the timescales of $\tau_{\text{tide}}/(2e^2)$. In that case, the orbits of the planets will become a little closer to the star than those without consideration of tidal effects. Owing to shorter timescales, the inner planets migrate faster, driving all of them out of MMR. Then, the configuration of KOI-152 forms and three planets are in near MMRs. This scenario may be suitable to account for the formation of other systems with planetary configurations like KOI-152.

Among 16 months data of Kepler, 242 target stars host two planet candidates, 85 with three, 25 with four planets, eight with five planets and one with six (Fabrycky et al. 2012). We examine all candidates and find that ten systems may have two pairs of the planets involved in near 2:1 MMRs, e.g., a near Laplacian resonance configuration. The orbital periods and their ratios are shown in Table 3¹. The ratios of orbital periods are all in the range of [1.83, 2.18], which may imply that they are likely to bear a formation scenario similar to KOI-152. In addition, the configuration of KOI-148 is close to the outcomes of Group 2-1 and 2-3 where two planets are simply trapped in 2:1 MMR, which demonstrates that the system may be formed when the star is older

¹ <http://archive.stsci.edu>

TABLE 3

THE ORBITAL PERIODS OF EACH PLANETARY CANDIDATE AND THE RATIOS BETWEEN THEM. P_{01} , P_{02} , P_{03} , AND P_{04} ARE, RESPECTIVELY, THE ORBITAL PERIODS OF THE PLANETS IN THE SYSTEMS.

ID	P_{01} (days)	P_{02} (days)	P_{03} (days)	P_{04} (days)	P_{01}/P_{02}	P_{02}/P_{03}	P_{03}/P_{04}
KOI							
152	52.09119	27.40415	13.484	-	1.9009	2.0323	-
571	13.34331	7.26733	3.886758	-	1.8361	1.8698	-
665	5.867973	3.07154	1.611912	-	1.9104	1.9055	-
733	11.34917	5.924992	3.132968	-	1.9155	1.8912	-
829	38.5596	18.64902	9.75222	-	2.0676	1.9123	-
898	20.08923	9.77059	5.16991	-	2.0561	1.8899	-
899	15.36813	7.11388	3.306569	-	2.1603	2.1514	-
1426	150.0341	74.91443	38.87641	-	2.0027	1.9270	-
1860	12.2094	6.3194	3.0765	-	1.9321	2.0541	-
1895	32.1349	17.2812	8.4575	-	1.8595	2.0433	-
935	87.6464	42.6329	20.85987	9.6168	2.0558	2.0438	2.1691
148	42.89554	9.67374	4.777978	-	4.4342	2.0247	-

than the case of KOI-152 with $\dot{M} = 2 \times 10^8 M_{\odot} \text{ yr}^{-1}$.

Marcy et al. (2001) revealed that there were two giant planets involved in a 2:1 MMR orbiting the star GJ 876. However, after the fourth planet was discovered in the GJ 876 system, the previously known 2:1 MMR configuration then becomes a Laplacian resonance configuration, where three planets are trapped into a 4:2:1 MMR with the resonant angles librating at 0° , respectively, differing from the Galilean moons of Jupiter in a libration at 180° (Rivera et al. 2010). In such configurations, a planetary system will remain stable at least one billion years. A great many of previous works had investigated the dynamics and stability of the system consisting of three planets at then (Ji et al. 2002, 2003; Zhou et al. 2005; Zhang et al. 2010). From the former results, we learn that the migration scenario may be responsible for the formation of two giants which is locked into 2:1 MMR. Thus under the same formation scenario for KOI-152, three planets may be also trapped into a 4:2:1 MMR,

showing a resemblance to those of GJ 876. Hence, we may reach a safe conclusion that the near Laplacian configurations are quite common in the planetary systems as also revealed by Kepler and our work may provide some substantial clues to the formation of such intriguing systems.

We thank the anonymous referee for good comments that helped to improve the contents of the manuscript. W.S. is supported by NSFC (Grants No. 10925313, 10833001) and China Postdoctoral Science Foundation (Grant No. 2011M500962). J.J.H. acknowledges the support by the National Natural Science Foundation of China (Grants No. 10973044, 10833001), the Natural Science Foundation of Jiangsu Province (Grant No. BK2009341), the Foundation of Minor Planets of Purple Mountain Observatory, and the innovative and interdisciplinary program by CAS (Grant No. KJZD-EW-Z001).

REFERENCES

- Aarseth, S. J. 2003, *Gravitational N-Body Simulations*, by Sverre J. Aarseth, pp. 430. ISBN 0521432723. Cambridge, UK: Cambridge University Press, November 2003.
- Barnes, R., Jackson, B., Raymond, S. N., West, A. A., & Greenberg, R. 2009, *ApJ*, 695, 1006
- Baruteau, C., & Masset, F. 2008, *ApJ*, 672, 1054
- Batalha, N. M., Rowe, J. F., Bryson, S. T., et al. 2012, *arXiv:1202.5852*
- Bodenheimer, P., Hubickyj, O., & Lissauer, J. J. 2000, *Icarus*, 143, 2
- Borucki, W. J., Koch, D., Basri, G., et al. 2010, *Science*, 327, 977
- Borucki, W. J., Koch, D. G., Basri, G., et al. 2011, *ApJ*, 736, 19
- Cresswell, P., & Nelson, R. P. 2006, *A&A*, 450, 833
- Fabrycky, D. C., Lissauer, J. J., Ragozzine, D., et al. 2012, *arXiv:1202.6328*
- Ford, E. B., Rowe, J. F., Fabrycky, D. C., et al. 2011, *ApJS*, 197, 2
- Goldreich, P., & Tremaine, S. 1979, *ApJ*, 233, 857
- Goldreich, P., & Tremaine, S. 1980, *ApJ*, 241, 425
- Haisch, K. E., Jr., Lada, E. A., & Lada, C. J. 2001, *ApJ*, 553, L153
- Hubickyj, O., Bodenheimer, P., & Lissauer, J. J. 2005, *Icarus*, 179, 415
- Ida, S., & Lin, D. N. C. 2004, *ApJ*, 604, 388
- Ida, S., & Lin, D. N. C. 2008, *ApJ*, 673, 487
- Ikoma, M., Emori, H., & Nakazawa, K. 2001, *ApJ*, 553, 999
- Ji, J., Li, G., & Liu, L. 2002, *ApJ*, 572, 1041
- Ji, J., Liu, L., Kinoshita, H., et al. 2003, *ApJ*, 591, L57
- Ji, J., Jin, S., & Tinney, C. G. 2011, *ApJ*, 727, L5
- Koenigl, A. 1991, *ApJ*, 370, L39
- Kley, W., & Crida, A. 2008, *A&A*, 487, L9
- Kley, W., Bitsch, B., & Klahr, H. 2009, *A&A*, 506, 971
- Kokubo, E., & Ida, S. 2002, *ApJ*, 581, 666
- Kretke, K. A., & Lin, D. N. C. 2007, *ApJ*, 664, L55
- Kretke, K. A., Lin, D. N. C., Garaud, P., & Turner, N. J. 2009, *ApJ*, 690, 407
- Lee M. H., & Peale S. J. 2002, *ApJ*, 567, 596
- Lin, D. N. C., & Papaloizou, J. C. B. 1993, in: E.H. Levy & J.I. Lunine (eds.), *Protostars and Planets III*, (Tucson: Univ. Arizona)
- Lin, D. N. C., Bodenheimer, P., & Richardson, D. C. 1996, *Nature*, 380, 606
- Lissauer, J. J., Ragozzine, D., Fabrycky, D. C., et al. 2011, *ApJS*, 197, 8
- Masset, F., & Snellgrove, M. 2001, *MNRAS*, 320, L55
- Marcy, G. W., Butler, R. P., Fischer, D., et al. 2001, *ApJ*, 556, 296
- Mardling, R. A., & Lin, D. N. C. 2004, *ApJ*, 614, 955
- Natta, A., Testi, L., & Randich, S. 2006, *A&A*, 452, 245
- Paardekooper, S.-J., & Papaloizou, J. C. B. 2008, *A&A*, 485, 877
- Papaloizou, J. C. B., & Terquem, C. 2010, *MNRAS*, 405, 573
- Pollack, J. B., Hubickyj, O., Bodenheimer, P., et al. 1996, *Icarus*, 124, 62
- Pringle, J. E. 1981, *ARA&A*, 19, 137
- Rasio, F. A., & Ford, E. B. 1996, *Science*, 274, 954
- Rivera, E. J., Laughlin, G., Butler, R. P., et al. 2010, *ApJ*, 719, 890
- Sano, T., Miyama, S. M., Umebayashi, T., & Nakano, T. 2000, *ApJ*, 543, 486
- Shakura, N. I., & Sunyaev, R. A. 1973, *A&A*, 24, 337
- Steffen, J. H., Batalha, N. M., Borucki, W. J., et al. 2010, *ApJ*, 725, 1226
- Tanaka, H., Takeuchi, T., & Ward, W. R. 2002, *ApJ*, 565, 1257
- Terquem, C., & Papaloizou, J. C. B. 2007, *ApJ*, 654, 1110
- Vorobyov, E. I., & Basu, S. 2009, *ApJ*, 703, 922
- Ward, W. R. 1997, *Icarus*, 126, 261

- Wang, S., & Zhou, J. L. 2011, ApJ, 727, 108
- Zhang, N., Ji, J., & Sun, Z. 2010, MNRAS, 405, 2016
- Zhou, J. L., Aarseth, S. J., Lin, D. N. C., & Nagasawa, M. 2005, ApJ, 631, L85
- Zhou, J. L., & Lin, D. N. C. 2008, IAU Symposium, 249, 285